

A novel method for vegetation encroachment monitoring of transmission lines using a single 2D camera

Junaid Ahmad · Aamir Saeed Malik ·
Mohd Faris Abdullah · Nidal Kamel ·
Likun Xia

Received: 23 June 2013 / Accepted: 22 July 2014 / Published online: 14 August 2014
© Springer-Verlag London 2014

Abstract The dangerous, overgrown vegetation/trees under high voltage transmission lines right-of-ways (ROWs) have caused severe blackouts/flashovers due to interference with power lines which leads to short circuiting among the conductors. Therefore, these dangerous encroachments are monitored periodically along the electrical distribution networks ROWs through visual inspection, or by airborne system. Each of these methods has its own attributes and limitations and have proved to be costly, time consuming and not much accurate. In these circumstances, it is necessary for the electrical utilities to review their vegetation management practices so as to avoid incidents of unintended encroachments. In tropical countries, overgrown vegetation is a common cause for power line failure. This paper proposes an innovative concept of utilizing a single camera for monitoring dangerous vegetation (trees, shrubs and plants, etc.) under transmission lines ROWs. The main focus is on using an imaging device (camera) integrated on each transmission pole to automate

inspection for the vegetation encroachments endangering the transmission lines. These cameras are envisioned to be connected wirelessly to each other, forming a series of wireless camera networks that can be monitored remotely. A single camera mounted on power poles acquires images and sends them wirelessly to the base station. At base station, algorithm (software) trained by image processing and pattern recognition techniques is used to identify (height, depth, and width of encroached vegetation, etc.) excess vegetation encroachments within and outside ROWs. The performance evaluation of a real time developed test-bed scenario proves the feasibilities of integrating the method for transmission line maintenance.

Keywords Transmission lines · Blackouts/flashovers · Right-of-ways · Encroachments · Image processing · Pattern recognition · Single camera

1 Background

The overgrown vegetation under high voltage (HV) overhead lines right-of-ways (ROWs) has caused severe blackouts/flashovers due to interference with operation circuits which leads to short circuiting among the conductors. As an example, the 2003 US–Canadian blackout occurred due to inadequate tree trimming which resulted in three 345 kV lines and one 138 kV line outages, causing huge financial losses for electric utility companies operating in North America, and damages to consumers [1]. In the same year, a very immense power outage occurred in Italy when tripping of a major HV line between Italy and Switzerland was caused by a tree flashover. In Malaysia nearly about 66 % of country area is covered with forests, and numerous blackouts had been recorded due to

J. Ahmad (✉)
Department of Electrical Engineering, University of Engineering
and Technology, KSK Campus, Lahore 54890, Pakistan
e-mail: junaid-ahmad@uet.edu.pk

A. S. Malik · M. F. Abdullah · N. Kamel · L. Xia
Department of Electrical and Electronic Engineering, Universiti
Teknologi Petronas, Bander Seri Iskander, Tronoh 31750, Perak,
Malaysia
e-mail: aamir_saeed@petronas.com.my

M. F. Abdullah
e-mail: mfaris_abdullah@petronas.com.my

N. Kamel
e-mail: nidalkamel@petronas.com.my

L. Xia
e-mail: likun_xia@petronas.com.my

vegetation intrusions. Between years 2005 and 2008, the power line blasts occurred because of interaction of overhead lines with excess vegetation (trees) in Sarawak in East Malaysia [2]. Outages occur when trees and HV lines come closer to one another passing the minimum allowed distance. Due to bad weather conditions including rain, wind and storm, etc., these vegetations can also strike the power line sag, or sometimes hot weather can result in sagging of HV transmission lines into tree branches causing line outages. Hence, it is necessary and crucial for electric utilities to ensure reliability and safety of overhead lines against endangering encroachments.

The traditional method for inspecting HV lines is visual field survey, whereby a team is deployed to inspect the power lines either by pole climbing or using vehicles. For pole-climbing, linesmen climb up a pole with computer having information regarding the components at that pole. This method is less accurate due to judgmental errors by humans for vegetation that appears to be in safe clearances but could be dangerous during bad weather conditions, e.g., heavy rain, wind and storm, etc. Other methods of monitoring are based on aerial inspection which includes: helicopter surveillance, videography by means of stereoscopy imaging and airborne LiDAR scanners have been explained thoroughly in terms of scientific contents about the particular problems and technical difficulties, both from data collection (i.e. sensor evaluation) and data analysis in [3]. Helicopters mounted with surveillance cameras are used to inspect the region with transmission line network [4]. This method is ambiguous for a non-uniform terrain due to changing perspective of target via random motion of camera in vertical direction as in [5]. However, the airborne LiDAR scanning is an optical remote-sensing technique that uses the scattering of light to find the range and other information of the distant object. After taking the data from LiDAR, it is mapped on the geographical information system (GIS) integrated with computer to recover the original coordinates and 3D view of the scenario [6]. By using LiDAR, an average of about 100 km of data is collected per day and no permission from the land owners is needed. In general, the data are processed in AutoCAD or other software packages like PLS-CADD, ESRI and Small World, etc. Uneven hovering of airborne vehicle causes ambiguities in the data recorded by LiDAR and consequently the software used for 3D tracking of transmission line can produce ambiguous model of the scene. Aerial stereoscopy technology captures images of ground from an elevated position by means of stereovision [7, 8]. Depending on the altitude, it allows to capture the images with appropriate resolution. However, low flight altitude (<500 m), difficulty in obtaining flight permission, high cost and low accuracy are the main disadvantages of stereo videography.

Each of these methods has specific attributes. But none of these methods provide a satisfactory way for efficient monitoring (with respect to accuracy, time and cost) as tabled in [3]. LiDAR technique may provide accurate results (about 70 %) but still it is very expensive to use. Presently, US is spending about \$2 billion per annum on using LiDAR and mapping surveys of HV lines for vegetation management in North America. Currently, the utility companies all over the world inspect their power distribution networks on regular intervals using visual field survey or airborne technologies (e.g., LiDAR). In this paper, we have proposed a single camera-based automated, non-airborne method that uses an image-processing platform to monitor the vegetation encroachments ROWs.

2 Integration of single camera on each transmission pole ROWs

To automate the inspection of overhead HV lines, a single camera is deployed to examine transmission lines for vegetation encroachments. Those single cameras are installed along the transmission poles ROWs that can be interlinked wirelessly to one another forming a monitoring network. The images captured by those cameras are transmitted to base station wirelessly where they are processed to identify whether the vegetation are in danger zone or not. In the proposed method, a single scene image is captured with appropriate resolution to:

- A. Detect the encroached vegetation within and outside ROWs boundary carrying the transmission lines.
- B. Estimate the 3D localization of the encroached trees in real world coordinates.
- C. Calculate the absolute height of trees, distance between the encroached vegetation and transmission poles and distance between transmission lines and excess vegetation outside ROWs.

To simulate the scenario, an experimental prototype containing a single camera (a wireless camera kit from Intel Crossbow that contains an IMB400 camera board which incorporates an OV7670 imaging sensor that is capable of acquiring RGB color images having resolution 640×480 pixels is used to capture the data (images) and sends them wirelessly to gateway PC <http://www.memscic.com>) and a set of modeled transmission lines is used. The wireless protocols and various communication topologies that can be utilized by those wireless cameras (integrated on HV poles) to communicate with one another over a long distance (since the distance between HV poles is normally maximum up to 400 m) to transmit data to base station are explained in [9–12] and thus need not to be discussed much in detail as those authors have contributed much on

multimedia communications. The band for communication among those cameras that can be used is 2.4 GHz as it is un-registered globally. The power issues for the cameras can be met by using solar battery, as it provides a longer life time due to its continuous charging, and it is a cost-effective solution for devices, sensors and cameras used outdoors [13]. Those cameras are firmly sealed in a plastic-type coating and are covered with a windshield to avoid any problem from electromagnetic (EM) radiations of HV lines and bad weather (including wind, storm and heavy rain, etc.). Whereas, the main task is to develop an algorithm using image processing and pattern recognition techniques to monitor the dangerous vegetation in data (image frames) received at the base station. After that,

operators at base station will order the trimmers to cut-off the vegetation wherever it is required.

3 Methodology to detect encroached vegetation ROWs

Some images showing vegetation surrounding overhead lines captured from various locations in Ipoh (Malaysia) are shown in Fig. 1. Figure 2 shows various images of a model for miniature overhead transmission line with the lens of the camera located at three fourth of height of the pole. The modeled overhead lines are built with spans of 0.5 and 1.0 m. A model of encroaching vegetation is positioned at front and back of the pole and left/right side



Fig. 1 a 22 kV overhead power lines along Lumut–Ipoh highway. b Overhead lines passing through fields in Ipoh. c The encroachments due to uneven dispersion of power lines. d Overhead lines in dense residential area

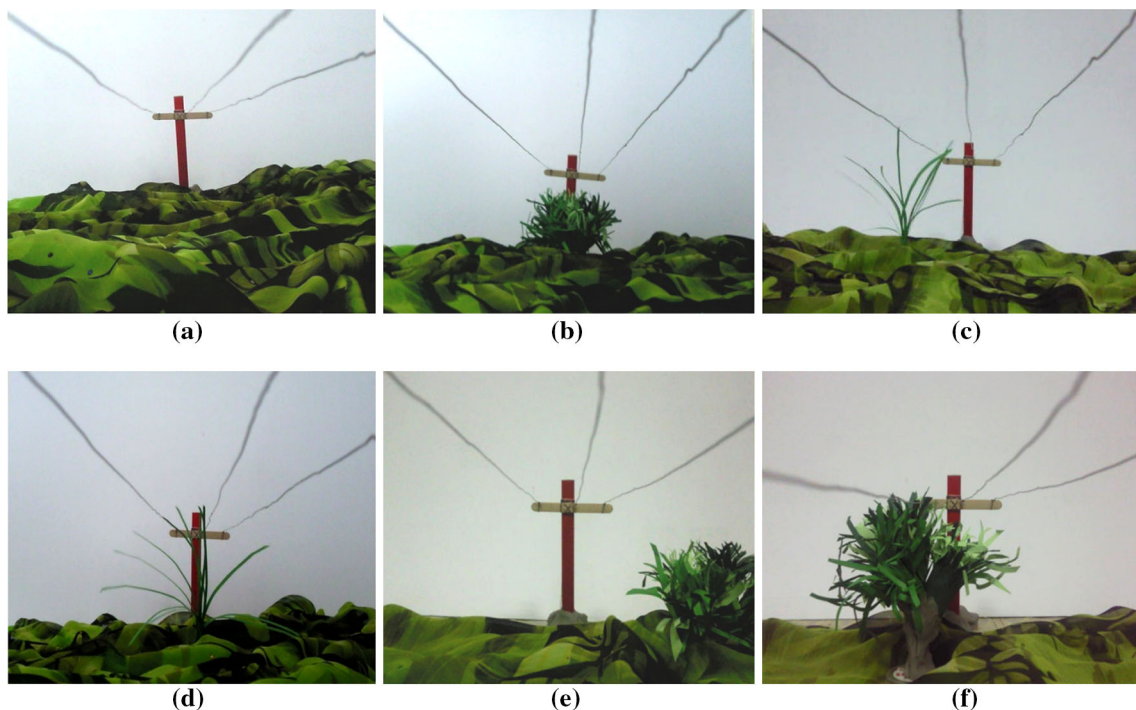


Fig. 2 a Overhead line clearance from encroachment. b Potential encroachment from beneath the overhead lines. c Leafy-type vegetation encroachment from the side. d Leafy-type vegetation

encroachment from underneath the line. e Potential, bushy-type vegetation encroachment from side. f Bushy-type vegetation encroachment from underneath

of the camera's range of view, with varying distances to the pole and overhead lines. A picture of overhead lines clear of vegetation encroachment is shown in Fig. 2a, while Fig. 2b shows a potential encroachment from beneath the lines which consists of bushy vegetation. Although not fully an encroachment to the line, it has potential to grow and disrupt the line. Figure 2c shows encroachment of leafy vegetation, with the leafy vegetation positioned slightly to left side of the pole in view. Whereas Fig. 2d demonstrates encroachment of leafy-type vegetation from the front of the pole in view, Fig. 2e shows potential bushy-type vegetation encroachment from the sides. A full encroachment of bushy-type vegetation, located at the front of the pole in view is shown in Fig. 2f.

The objective of this research is to develop an imaging algorithm that can easily identify vegetation that can harm HV lines ROWs. The overall procedure is divided into four stages. The first stage includes the acquisition of initial reference and scene image frames. The second step is the filtering and identification of weather conditions, whereas the third and fourth stages are to identify transmission poles, and to detect the level of encroached vegetation. If

the vegetation is encroached above a certain level (height) an alarm will be made to the operators residing at the base station to trim the endangering encroachments. The framework for the algorithm is divided into four main steps given below and shown in Fig. 3:

- A. Initialization by reference and scene images,
- B. Pre-processing (filtering and weather identification),
- C. Identification of transmission pole,
- D. Monitoring the level of encroached vegetation.

3.1 Initialization by reference and scene images

The first step in Fig. 3 is to capture some initial reference frames. These initial reference frames are acquired when the trimmers come and cut off the vegetation to a zone out of danger within and outside ROWs. Those reference frames are acquired every five minutes (from 9 a.m. to 5 p.m.) for about first initial 10 days after trimming as there will be almost no change in the scene since vegetation growth is relatively a slow process regardless of the weather conditions. The criteria for capturing the reference

Fig. 3 Flow diagram for algorithm framework

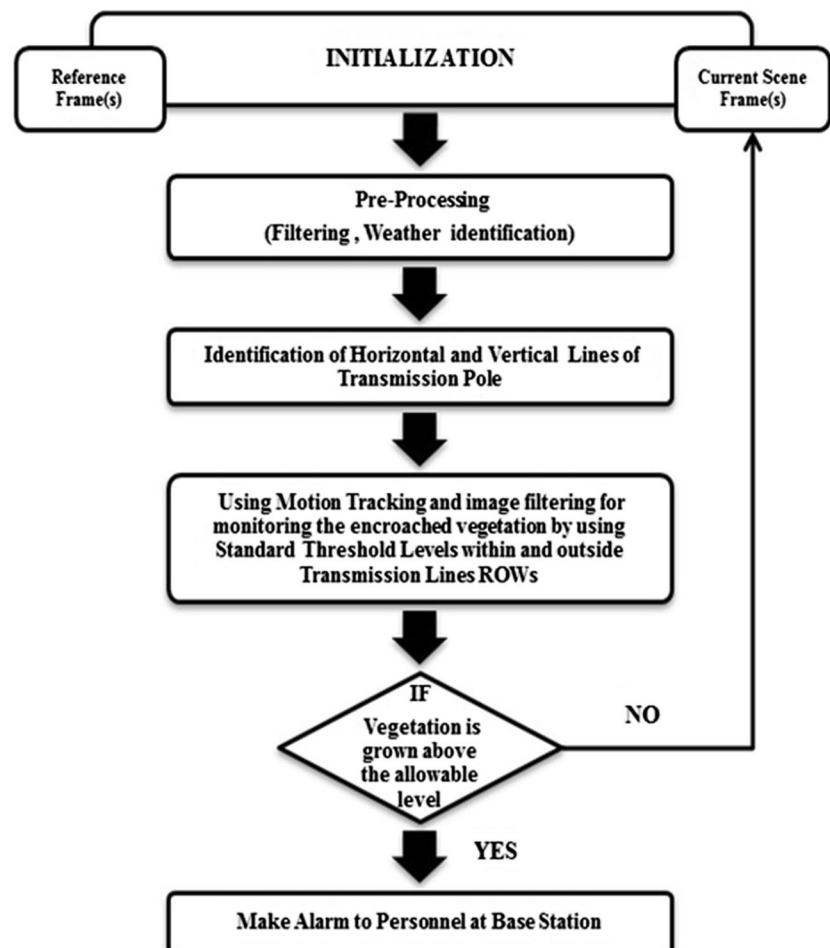
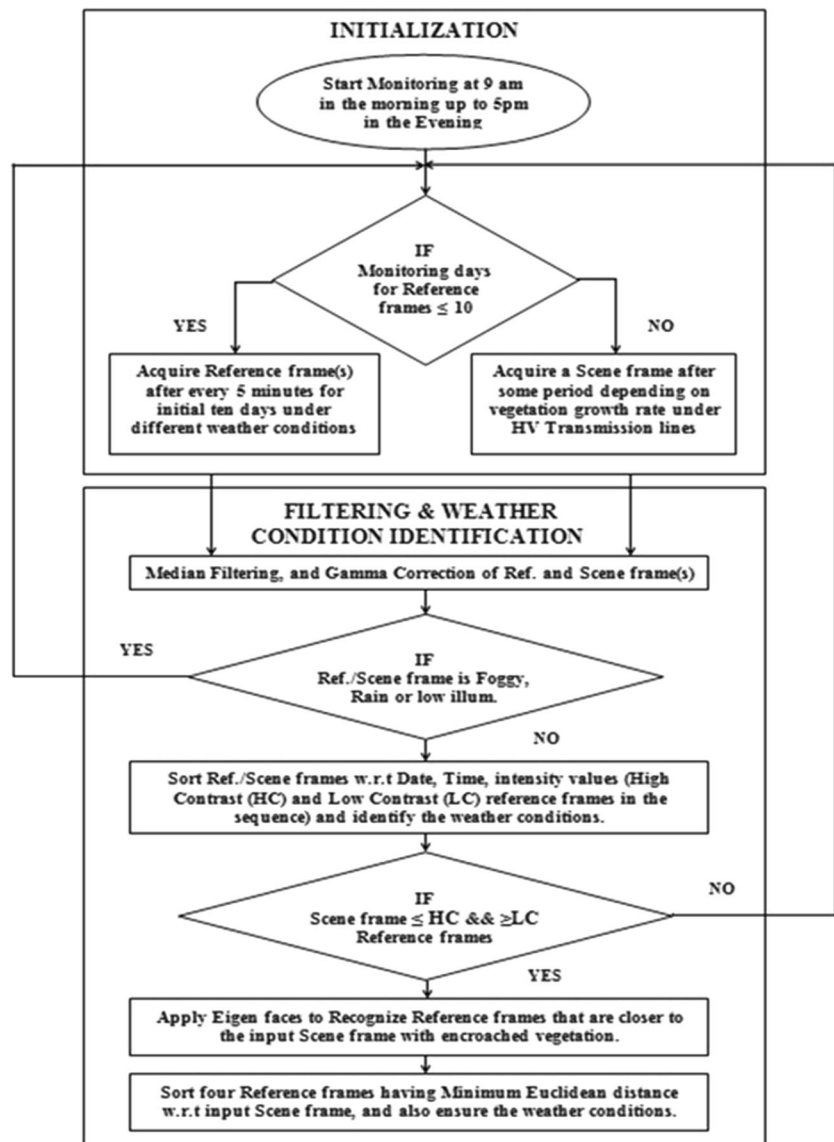


Fig. 4 Initialization and pre-processing (filtering weather and condition identification)



frames vary with weather conditions, e.g., in our case, Malaysia is a tropical country and weather changes abruptly but temperature remains warm throughout the year, unlike other parts of the world where the weather is hot in summer and cold in winter. The image frames acquired after 10 days will be considered as scene frames that will be analyzed for detection of vegetation encroachments as shown in Fig. 4.

3.2 Pre-processing (filtering and weather identification)

Sunny, rainy, foggy, etc., weather conditions are identified in all the reference and scene image frames in order to only consider the image frames with appropriate illumination. This is because handling uneven illumination for image-processing applications operating outdoors such as video

surveillance, environmental control, and robotic vision is a very challenging task. To overcome this problem, pattern recognition techniques are used to extract features for the automated classification of weather (illumination) conditions in the images. Figure 4 shows the incoming images (either reference or scene) to be firstly filtered by a median filter of window size 3×3 to remove any unwanted noise. Then gamma correction is used to adjust the brightness in those frames.

3.2.1 Detection of rain

The rainy images are identified by detecting the raindrops on windshield of the camera mounted on HV pole in real-time environment by extracting the raindrop features having the following characteristics [14]:

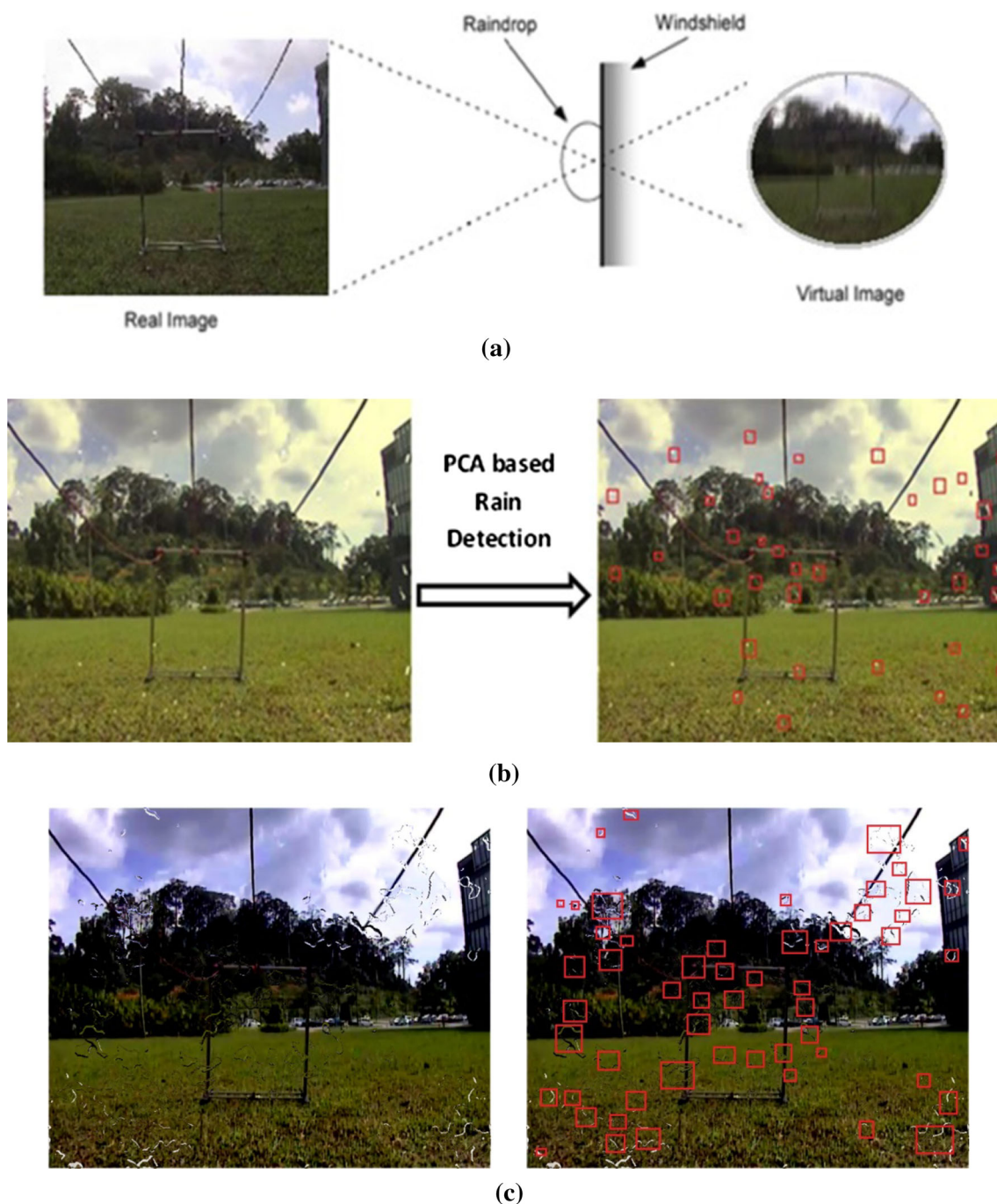


Fig. 5 **a** Image seen through the windshield covered with raindrop. **b** Detection of raindrops in fair, rainy weather. **c** Raindrops identified in heavy rain with a threshold $S(K) \geq 0.74$

- Uniform in shape (raindrops appear to be circular in shape if seen through the windshield),
- Refraction of light (being clear and colorless refraction takes place due to varying background).

We have used this method which has been published in [14]. Figure 5a shows a rainy image through the windshield. Principal component analysis (PCA) is used to recognize the pattern of raindrops on the windshield of

camera by matching raindrop templates (frames) with the incoming reference or scene frames [14]. At first M templates (frames with raindrops on the windshield) each of width (W) and height (H) are captured for training, and represented by one-dimensional vectors, that are normalized to unit vectors given as: $x_i = (x_1, x_2, \dots, x_N)^T$, where $N = W \times H$. Let $X = [x_1, x_2, \dots, x_M]$ be a matrix of M randomly selected vectors from the test images, and its

covariance matrix be $Z = XX^T$. We compute the largest eigenvalues Q of Z and its corresponding eigenvectors $\{e_1, e_2, \dots, e_Q\}$. The rain detection is done by computing the correlation which finds the degree of similarity between the one-dimensional normalized test (reference or scene) image and the eigenvectors (raindrops in template frames). If K is the test image area, then $S(K)$ is given by:

$$S(K) = \sum_{q=1}^Q (K, e_q)^2 \tag{1}$$

The frame is detected as rainy if $S(K)$ is greater than a threshold (which is set to 0.5 owing to drastic raindrop properties as compared to ordinary images) by computing the similarity between the eigenvectors. Figure 5b and c show results for the detection of raindrops on images (reference and scene images) captured under different rainy environments.

3.2.2 Detection of fog

Similarly, we used the method published in [15] for prediction of foggy weather that utilizes the ‘dark channel prior model’ to measure the fog level in an image. This dark channel is computed for first prior reference frame which will be a clear image observed visually at base station. The image of dimension $W \times H$ is further divided into $K \times L$ patches. We can get the darker intensity value in each patch simply by finding the minimum of all. After that the dark channel prior of this clear image is given by [15]:

$$L_N^{\text{dark}} = \{L_1^{\text{dark}}, L_2^{\text{dark}}, \dots, L_n^{\text{dark}}\} \tag{2}$$

where n is the number of patches. After that, we use the above-mentioned method to compute the dark channel of the next new incoming reference or scene frame as [15]:

$$C_N^{\text{dark}} = \{C_1^{\text{dark}}, C_2^{\text{dark}}, \dots, C_n^{\text{dark}}\} \tag{3}$$

Next, the difference between the two dark channels of the corresponding patches is calculated. The average difference is computed as [15]:

$$D = \frac{\sum_{i=1}^n |C_i^{\text{dark}} - L_i^{\text{dark}}|}{n} \tag{4}$$

At the end, a threshold (thresh) makes a decision whether the image is foggy or not. If $D \geq \text{thresh}$ then the frame is identified as foggy. Since, we are identifying the amount of whiteness in an obscured foggy image; therefore threshold (thresh) is set to 100 owing to average differencing of foggy image (with majority pixels having intensity value 255) from clear image having sufficient illumination even during intense sunshine in the presence of greenery.

3.2.3 Identification of similar reference and scene frames

Any frame detected to be rainy or foggy will be discarded and our algorithm will wait for the next frame (reference or scene) as in Fig. 4. The reference frame (for initial 10 days as in step 1) free from fog and rain having sufficient illumination will be sorted as a dataset (training set) at base station with respect to date, time, weather, and contrast. After 10 days till the time of vegetation encroachment, the scene images captured are also filtered and detected to be either rainy, foggy or low illumination (average intensity value less than 100 due to green color of vegetation which is common in tropical countries all the year). After that, scene image is selected having the average intensity value ranging between the values of highest contrast (HC) and lowest contrast (LC) from a dataset of reference images.

After the identification of acceptable scene image, an automated algorithm is developed to sort out at least two to three reference frames from the entire dataset (reference frames) having the same illumination (weather) as captured scene image. This is done by using PCA, which retains the variation in data as much as possible [16, 17]. Each reference/scene image taken is an 8-bit array of size $W \times H$, which can also be considered as a column vector having dimension $(W \times H) \times 1$. Let $I_1, I_2, I_3, \dots, I_Z$ be the training dataset of reference frames acquired for 10 days in an outdoor environment under varying illuminations from 9 a.m. in morning up to 5 p.m. in evening as shown in Fig. 6. Next compute the mean of the frames in the training dataset, and difference of each image frame (of the dataset) from the mean vector to form a matrix $A = [\Phi_1, \Phi_2, \Phi_3, \dots, \Phi_Z]$, where $(W \times H) \times Z$. After that find the covariance matrix $C = AA^T$, and compute its eigen vectors (v_1, v_2, \dots, v_X) and eigen values ($\lambda_1, \lambda_2, \dots, \lambda_X$). The dimensionality is reduced from X to Y space by keeping only the eigen vectors corresponding the largest eigen values:

$$\hat{I}_i - \bar{I} = \sum_{u=1}^Y b_u^i v_u^i \text{ where } Y < X, i = 1, 2, 3, \dots, Z \tag{5}$$

Represented in form of a vector containing the weights as:

$$\Omega_i = [b_1^i \ b_2^i \ \dots \ b_Y^i]^T \tag{6}$$

Equation (6) describes the contribution of each reference frame in dataset, and is used to identify the illumination pattern of an input scene image with encroached vegetation. Repeat this procedure to find the vector containing the weights of scene image as:

$$\Omega = [b_1 \ b_2 \ \dots \ b_Y]^T \tag{7}$$

To find the reference frame similar to scene frame compute $e_r = \|\Omega - \Omega_i\|^2$, which is the Euclidean distance

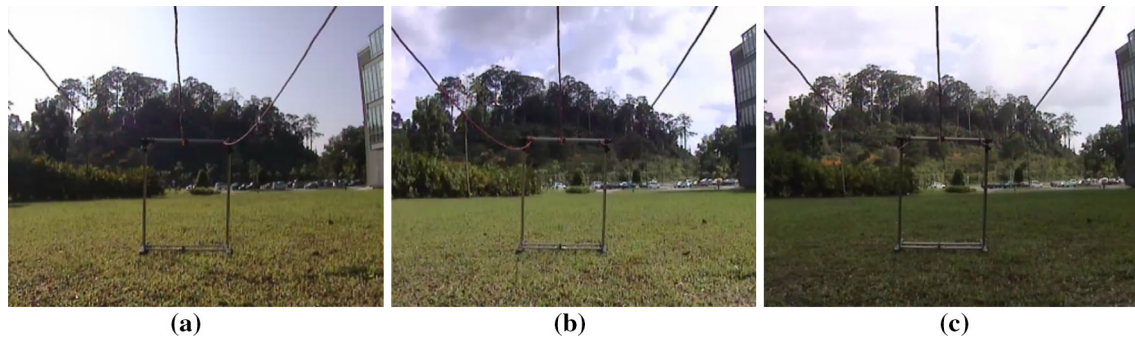


Fig. 6 **a** Transmission line reference frames under intense sunshine at 12 pm in the afternoon. **b** Reference frames at 3 pm under normal sunshine. **c** Reference frames under cloudy environment at 5 pm in evening

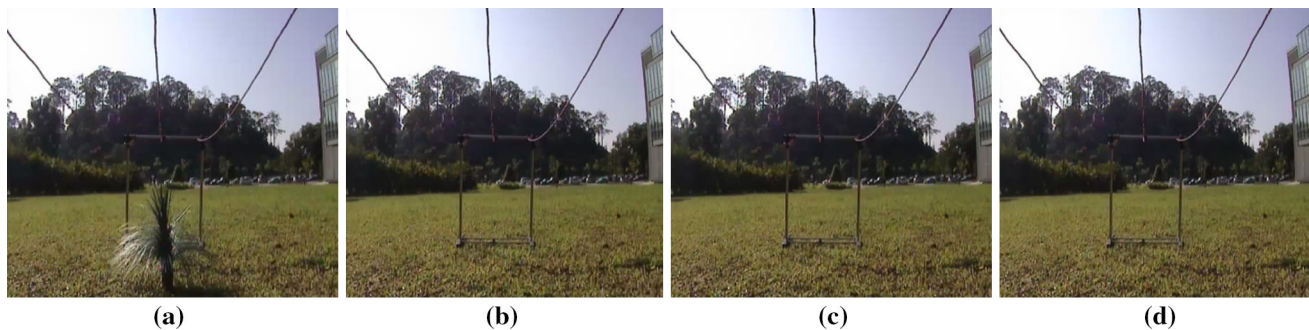
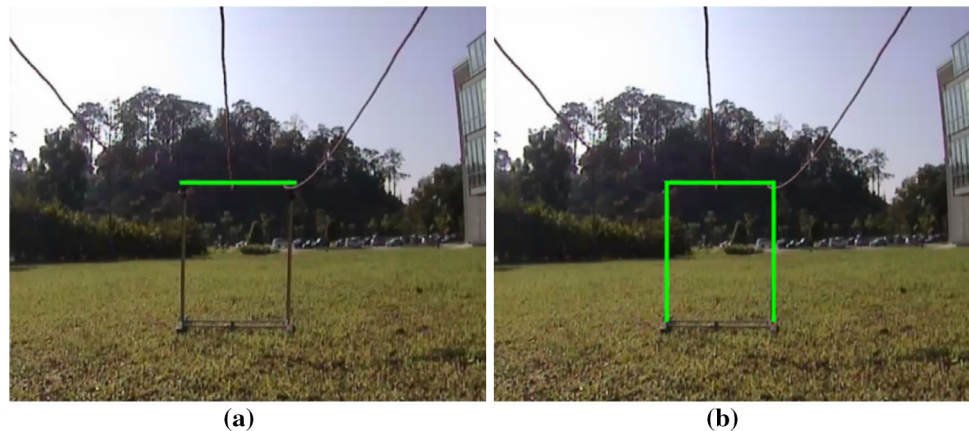


Fig. 7 **a** Scene image of a transmission line model having a tree. **b** Three sorted reference frames close to the scene image in illumination

Fig. 8 **a** Identification of horizontal lines of far away pole. **b** Identification of vertical lines



between the weights of scene and reference frames of training dataset. Two to three reference frames that are closer (having same illumination) to scene frame with minimum distances are sorted out in ascending order by using this procedure as in Fig. 7.

3.3 Identification of transmission poles

The HV transmission poles have different structures in power engineering. But every power pole consists of horizontal and vertical lines regardless of its power rating [18]. Therefore, we identify the horizontal and vertical

lines of far away poles by using the Hough transform (as in [19, 20]) for one reference frame out of sorted ones to determine the horizontal and vertical thresholds to monitor the dangerous vegetation ROWs as in Fig. 8. Hough transform is used for feature detection especially straight lines [21, 22]. It states that n number of co-linear points on a straight line in x - y plane correspond to n number of straight lines passing through a single point in parameter space. For computational reasons, Rho (ρ)-theta (θ) space is used in Hough Transform instead of parameter space. The detection of horizontal lines and threshold is given below as:

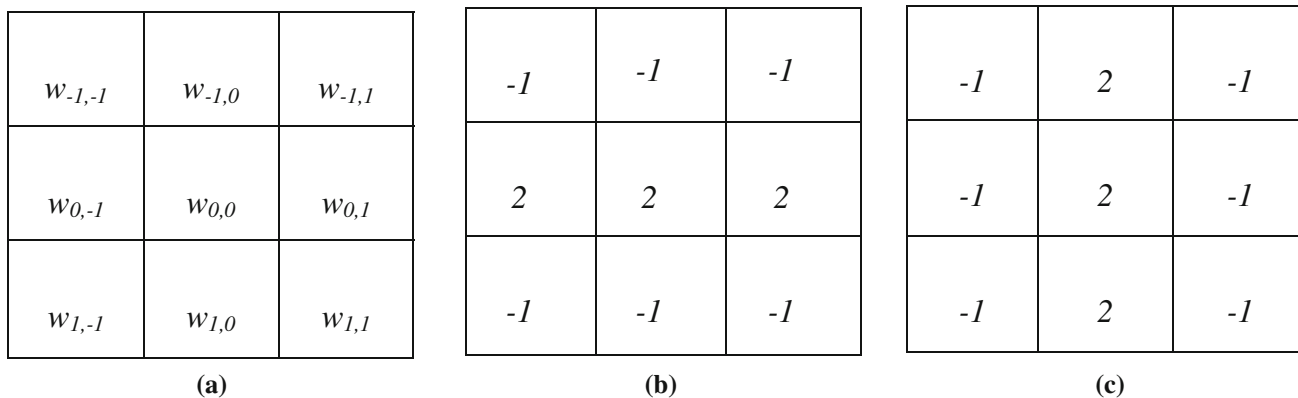


Fig. 9 a Coordinate arrangement of 3 × 3 masking coefficients, b horizontal mask, and c vertical mask

- Filter (convolve) the reference image $I_R(x,y,t_i)$ with horizontal mask as in Fig. 9b to find out the candidates for horizontal lines, where t_i is any time instant.

$$R(x, y) = w(x, y) \otimes I_R(x, y) = \sum_{n=-1}^1 \sum_{m=-1}^1 w_{n,m} I_R(x + n, y + m) \tag{8}$$

where $R(x, y)$ is the resulting filtered image, and $w(x, y)$ shows the masking coordinates as in Fig. 9a used to filter the reference image $I_R(x,y,t_i)$.

- Detect the edges by using the Sobel edge detector. $BW \leftarrow$ Apply Sobel Edge detector on $R(x, y)$

where BW is the output binary image.

- Apply Hough transform to BW , to identify horizontal lines in the image.

$L \leftarrow$ Apply Hough Transform on BW

- After that, only to detect the horizontal lines of far away pole and a suitable horizontal threshold to monitor the vegetation, a flowchart is shown in Fig. 10.

The above given flow diagram detects the horizontal lines, and threshold for the far away pole to monitor the vegetation. h_tresh is the horizontal threshold which shows the detected horizontal line of the pole as in Fig. 8a.

To detect vertical lines and thresholds for the same pole vertical mask shown in Fig. 9c is used to find candidates for vertical lines. Using similar steps, Hough Transform identifies vertical pole lines and two vertical thresholds to monitor the encroachments within and outside ROWs as given below:

$$v_tresh \leftarrow \text{Two vertical thresholds } [v_L, v_R]$$

where v_tresh consists of two vertical thresholds v_L and v_R , respectively, which represent the left and right most vertical lines (thresholds) of the pole as shown in Fig. 8b. Here it is important to mention that we did not emphasize

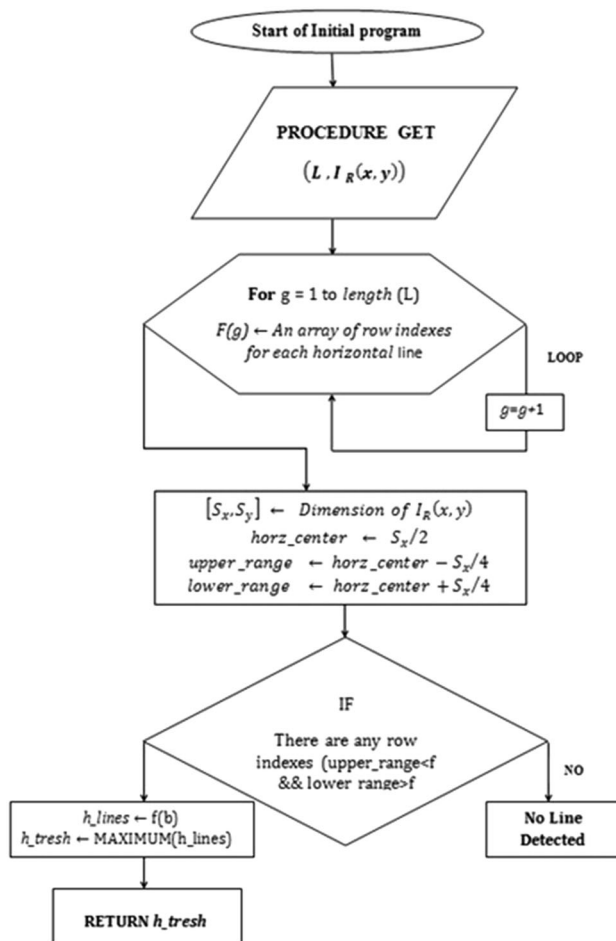


Fig. 10 Flow diagram to detect the horizontal lines and threshold of far away pole

to find out the threshold for power line sag to monitor dangerous encroachments, because HV conductors expand or stretch during hot and cold weather, respectively. Therefore, calculating the threshold for power line sag can produce ambiguous results.

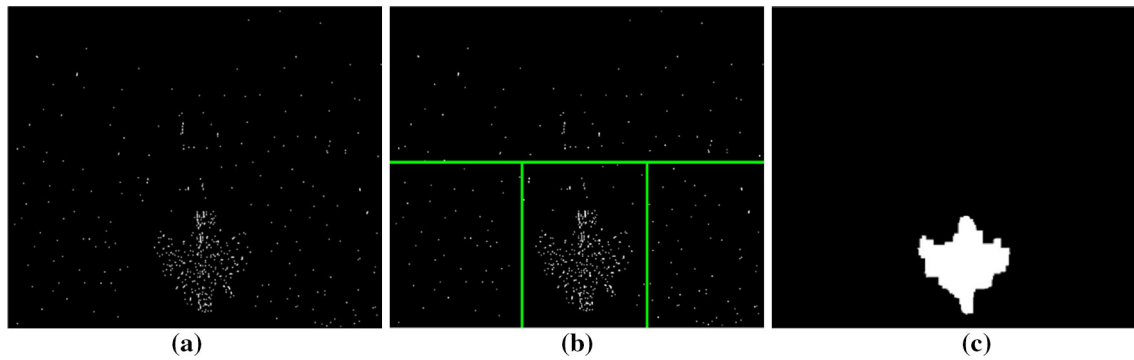


Fig. 11 **a** Subtracted-binarized scene image. **b** Utilization of horizontal and vertical threshold to discard uneven illuminations within and outside ROWs. **c** Use of morphological operator to discard unwanted pixels

3.4 Monitoring the level of encroached vegetation

After detecting the horizontal and vertical lines, tracking is used to detect the encroached vegetation in the scene image $I_S(x,y,t_j)$ with respect to reference images $I_R(x,y,t_i)$ as shown in Fig. 11. The vegetation tracking is done by filtering the scene image with Laplacian kernel to enhance the edges for better recognition of trees, and subtracting the reference frames from the scene, by using segmentation (background-subtraction) [23] that uses binarization as given below:

$$I_{RS}(x,y) = \begin{cases} 1 & \text{if } |I_S(x,y,t_j) - I_R(x,y,t_i)| > T \\ 0 & \text{otherwise} \end{cases} \quad (9)$$

Where T is the threshold for binarization and its value is set by taking the average intensity value of two to three reference frames (sorted by procedure as explained in Sect. 3.2.3) which are similar to the scene frame having same weather conditions irrespective of the encroached intrusions in them. The subtracted-binarized image will remain only with the data including vegetation that are encroached in the particular time duration since the reference images are taken. Figure 11a shows the subtracted-binarized image. It can be seen from the Fig. 11a that there are unwanted pixels because of small illumination variations. To overcome this, we have used horizontal and vertical thresholds to discard illumination effects outside ROWs as shown in Fig. 11b. Closing (dilation followed by erosion) of an image by ‘square’ element of size 5 is used as a morphological operator within ROWs to remove uneven appearances as shown in Fig. 11c.

The level of excess vegetation is determined by comparing the pixel values of binarized reference image with the subtracted-binarized image. This is done by placing few horizontal monitoring thresholds within and outside ROWs on the after-subtraction binarized frame. The procedure is explained in the flowchart as in Fig. 12. After determining

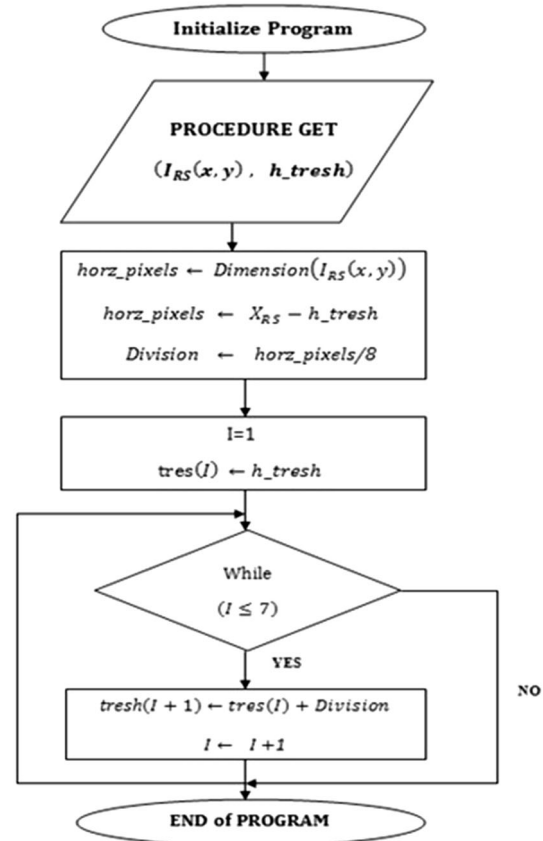


Fig. 12 Flow diagram to place the horizontal thresholds to detect the level of encroached vegetation

the horizontal threshold h_thresh in Sect. 3, the binarized image $I_{RS}(x,y)$ is further divided into eight monitoring thresholds as in Fig. 13 of this section. The Fig. 13a and b shows eight thresholds on the subtracted-binarized, and scene image presenting the zones lines having different colors as mentioned in Table 1. The height of HV transmission poles vary from 15 to 55 m depending upon the rating (including 500, 275, 33 kV etc.) of HV lines [24].

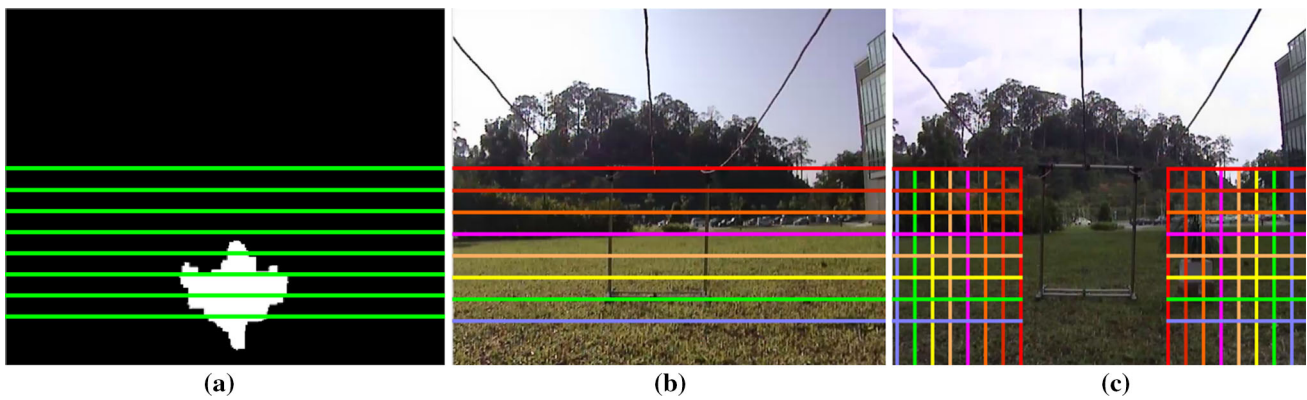


Fig. 13 **a** Thresholds placed on subtracted-binarized scene image to identify height of vegetation, **b** thresholds with different colors presenting various zones, **c** horizontal and vertical thresholds identify zone of encroached vegetation outside ROWs

Table 1 Monitoring thresholds represented by various colors

Zone line	Height of HV transmission pole w.r.t rating					Color
	500 kV (m)	275 kV (m)	132 kV (m)	66 kV (m)	33 kV (m)	
Alarming	55	45	35	25	15	Red
Dangerous	48	39	31	22	13	Orange
High	41	34	26	19	11	Brown
Critical	34	28	22	16	9	Purple
Tolerable	28	23	18	13	8	Light brown
Moderate	21	17	13	10	6	Yellow
Low	14	11	9	7	4	Green
Normal	7	6	4	3	2	Light blue

Table 1 shows zone lines with various colors relating to the height of HV poles having different rating. In the Fig. 13b, the highest threshold (zone) is the top most horizontal line of the pole; therefore if we assume the pole to be 500 or 275 kV then its height relating to this highest threshold will be 55 or 45 m as in Table 1. Therefore, any vegetation encroaching to this level will have a height nearly 55 or 45 m and the algorithm will indicate it to be in dangerous zone (where trees are interfering with the HV lines and may cause blackouts). As eight zones are used to monitor the HV lines, therefore practically each zone covers 7 or 6 m for 500 or 275 kV pole, respectively.

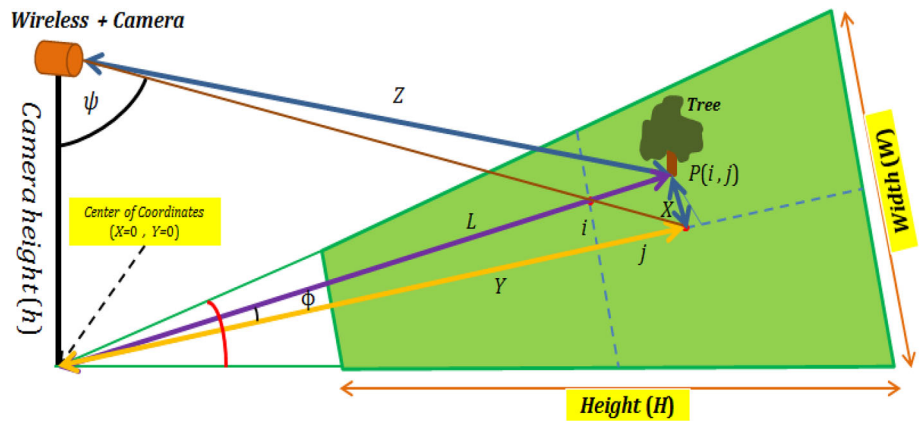
By using those monitoring zones, we identify the level of overgrown vegetation within and outside ROWs. In real-time environment, sometimes trees or shrubs appear to be in safe zone with respect to power lines outside ROWs. But during bad weather conditions those trees or shrubs can interfere/strike the power lines or even can fall on them. To overcome this problem, we monitor the vegetation outside (either on left or right side) ROWs. For this purpose, our algorithm tracks the level of vegetation to identify the zone and after that it tracks whether the vegetation is at the safe distance from power lines or not. The distance identification

is done by placing the vertical monitoring thresholds on left and right side ROWs in a similar fashion to horizontal ones. The overall status of the vegetation is found by comparing the level of vegetation with the distance of vegetation from the power lines. For example, if the level of vegetation is in danger zone and distance from power line is also in danger zone then the overall status of the vegetation would be dangerous and vice versa as in Fig. 13c.

3.5 Depth estimation of scene using triangulation

In this step, we have proposed a method based on analytical geometry to extract 3D coordinates of the scene. Depth from Triangulation (DfT) is used to find out the distance between the camera and trees (within and outside ROWs) in meters to ensure a safe distance between the transmission pole (camera) and the trees. This technique firstly extracts the overgrown vegetation in the scene by using background-subtraction shown in Fig. 13. Secondly, it identifies the ground location of vegetation in the scene because the centroid does not represent the true location of the image in 3D world coordinates. The proposed algorithm assumes a wireless camera installed at a known

Fig. 14 Computing the 3D coordinates of vegetation at location $P(i, j)$ using depth from triangulation (DfT)



height and a vertical angle on the pole; this is true for our conditions. In this model, the vegetation coordinates (X, Y, Z) are calculated given the camera height (h), the vertical angle (θ) and the field of view angle (FOV).

Figure 14 shows a camera setup where the trapezium green area shows the area covered by the camera view. The camera is installed at a height (h) from the ground with a vertical angle (θ) and the field of view angle (FOV). The horizontal field of view (FOV_H) for the IMB400 camera is 44.7° , and vertical field of view (FOV_V) is 60° [9]. Larger camera height covers larger viewing area, and field of view changes only with the zoom of camera and greater field of view means coverage of larger area. The vertical angle (θ) is constrained by the relationship $\theta < 90^\circ$, the trigonometric relation will produce erroneous results if the vertical angle exceeds the limit. The above mentioned parameters are generally known for all cameras and are calibrated during the installation process.

In Fig. 14, there is a tree (vegetation) at location $P(i, j)$ on the image having a width (W) and height (H). Thus, larger the image resolution, the finer the image element is and it can have more accurate localization of the tree location. However, if the size of the covered area is large (the camera height is large or the field of view is large), the resolution is reduced and the pixel element will be larger in size. Thus, there is a larger quantization error [25]. In Fig. 14, the rotation angle (ϕ) and the vertical angle (ψ) are computed for the tree located at point $P(i, j)$ as given below [25]:

$$\phi = \left(i - \frac{W}{2}\right) \times \left(\frac{FOV_H}{W}\right) \tag{10}$$

$$\psi = \theta + \left(\frac{H}{2} - j\right) \times \left(\frac{FOV_V}{H}\right) \tag{11}$$

Then the distances Y and X are computed using these two angles. Given the vertical angle (ψ) and the camera height (h) the distance (Y) in Fig. 14 is computed by using Eq. (12).

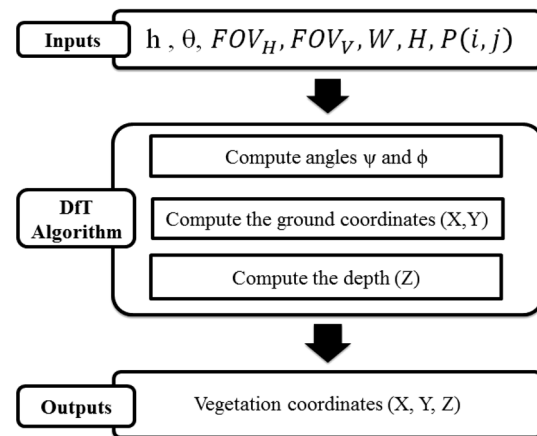


Fig. 15 Flow diagram of DfT Algorithm

$$Y = h \times \tan(\psi) \tag{12}$$

Then, given the distance (Y) and the rotation angle (ϕ), the distance (X) in Fig. 14 is computed using Eq. (13).

$$X = Y \times \tan(\phi) \tag{13}$$

Now by using the distances (X) and (Y) and the angles (ψ) and (ϕ), the 3D coordinates of the tree at point $P(i, j)$ are computed assuming that the center of coordinates is beneath the camera exactly as shown in Fig. 14.

$$L^2 = X^2 + Y^2 \tag{14}$$

$$Z^2 = h^2 + L^2 = h^2 + X^2 + Y^2 \tag{15}$$

$$Z = \sqrt{h^2 + X^2 + Y^2} \tag{16}$$

$$Z = h\sqrt{1 + \tan^2(\psi) \sec^2(\phi)} \tag{17}$$

X and Y in Eqs. (13) and (12), respectively, denote the vegetation coordinates with respect to ground of the scene. Z in Eqs. (16) and (17) is the depth of field or the actual distance between the vegetation and the camera. The algorithm for depth estimation of vegetation can be

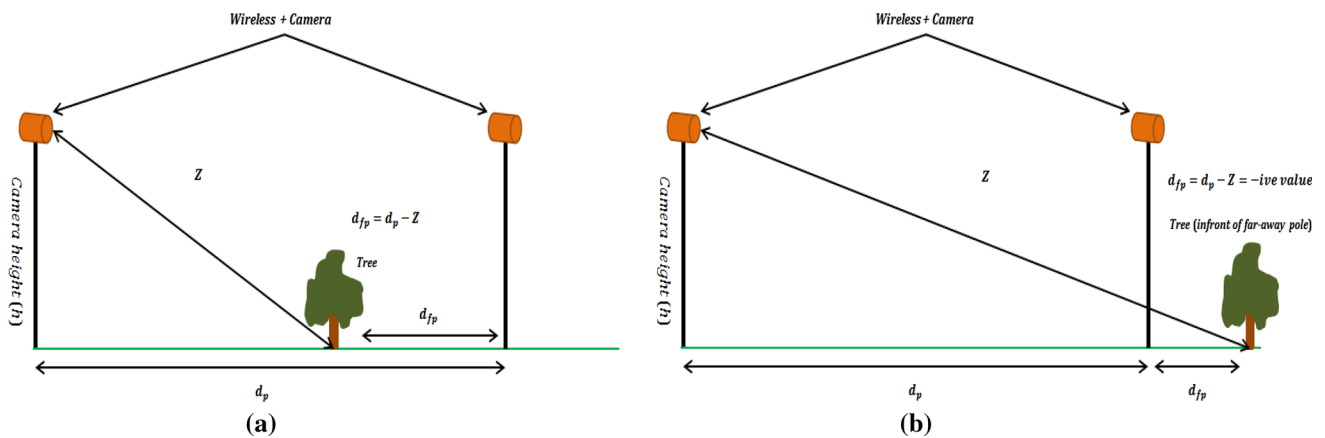


Fig. 16 **a** Distance between the far away pole and the tree, and **b** distance between the far away pole and the tree in front of pole

summarized in details in the steps below and also in the flow diagram of Fig. 15. The input parameters include: Camera intrinsic parameters [vertical field of view (FOV_v), horizontal field of view (FOV_H)], camera extrinsic parameters [camera height (h), camera vertical angle (θ)], and image parameters [width (W), height (H), and moving object location $P(i, j)$]. The algorithm as a whole computes the angles, world coordinates, and depth of field (Z). The output consists of $P(i, j) \leftrightarrow P(X, Y, Z)$.

The proposed technique finds out the distance between the camera (pole) and the trees. As the distance between the two poles is known so the distance of the tree from the far away pole can also be calculated as in Fig. 16a. For our conditions, the tree can be either on backside of the far away pole or in the front. By calculating the distance between the tree and the camera we can determine whether the tree is at the backside or in front of the far away pole as in Fig. 16b. One thing is that our algorithm can track only the trees that are fully in its field of view (FOV). By looking at Fig. 16b, it can be seen that the algorithm will find out accurate distance between camera and tree up to halfway distance in front of the far away pole. In Fig. 16b, the negative distance indicates that the tree is in front of the far away pole, and if the value is positive it means that the tree is at the back side of the pole as in Fig. 16a.

If the transmission network is installed on a hilly surface as in Fig. 17a, the cameras are placed on the similar pattern as the terrain. Placement of two cameras is solution to the problem where the terrain is highly non-uniform to overcome the blockage of whole scene as in Fig. 17b. The cameras are installed in a similar manner so that vertical angle of cameras with respect to terrain should be less than 90° to produce correct results. Similarly, two cameras will be used in region of highly non-uniform terrain to monitor those encroachments that may not be seen by camera on the far away pole due to blockage of the scene.

By using thresholding we were able to find out the zone of vegetation as in Table 1. Now, by finding out the depth and the 3D location of tree that are located on the ground the height of the tree can be computed by constructing a geometrical model using the bottom point and the top point of the object. Then similar triangles in the scene are used to compute the height. In Fig. 18, the ground distance ($Z1$) is computed using base point (BP) and the ground distance ($Z2$) is computed using the triangulation algorithm from top point (TP). Then by using similar triangles, the tree height (HE) is computed using equation 18.

$$HE = h \times \frac{Z2 - Z1}{Z2} \tag{18}$$

3.6 Identification of distance between HV lines and trees in vicinity using depth from triangulation (DfT)

In real-time environment, some vegetation outside ROWs appears to be in safe zone with respect to HV overhead lines. However, owing to bad weather those dangerous trees can strike or even fall on HV lines. Therefore, it is necessary to maintain a suitable clearance distance from those encroachments. To overcome this problem, distance between excess outside vegetation and HV transmission lines is determined. This is done firstly by monitoring the encroachments left and right side ROWs. For this purpose, the algorithm has already determined the level and actual height of vegetation as in fourth and fifth step, respectively. After that, the algorithm is used to identify the zone (dangerous, high, medium, etc.) whether the encroached vegetation (outside) is at the safe distance from power lines by placing the predetermined threshold levels.

After determining the zone of the encroached vegetation with respect to the HV lines and poles, a new analytical geometry is proposed as in Fig. 19 that will utilize data from the above triangulation based technique to find out the

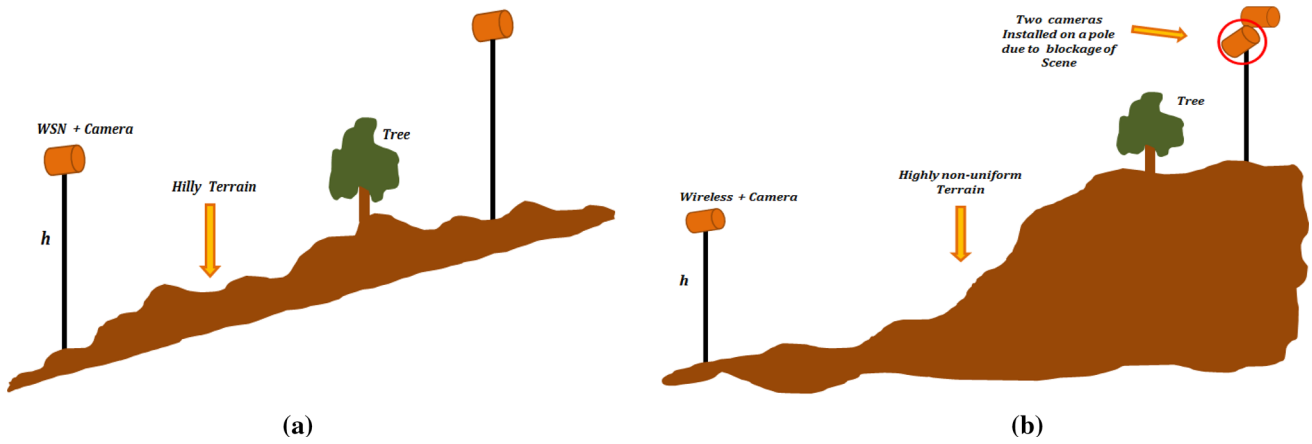


Fig. 17 **a** Wireless cameras installed on the poles in a similar manner as trainee. **b** Installation of two cameras on a pole passing through a highly non-uniform trainee due to blockage of scene

Fig. 18 Computing height of the tree

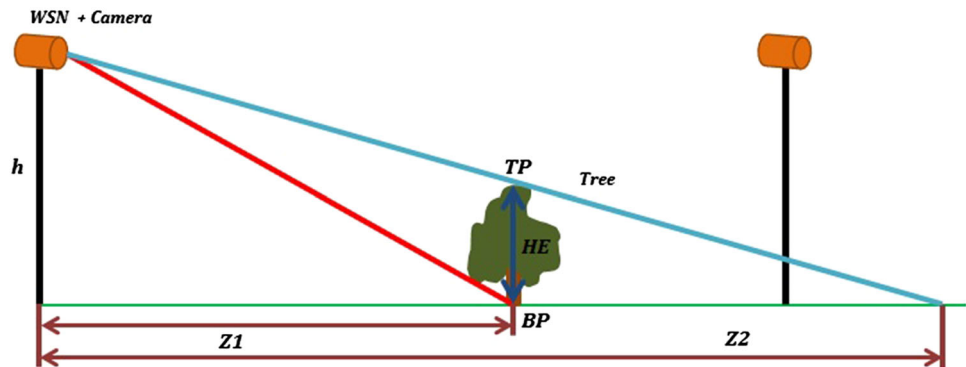
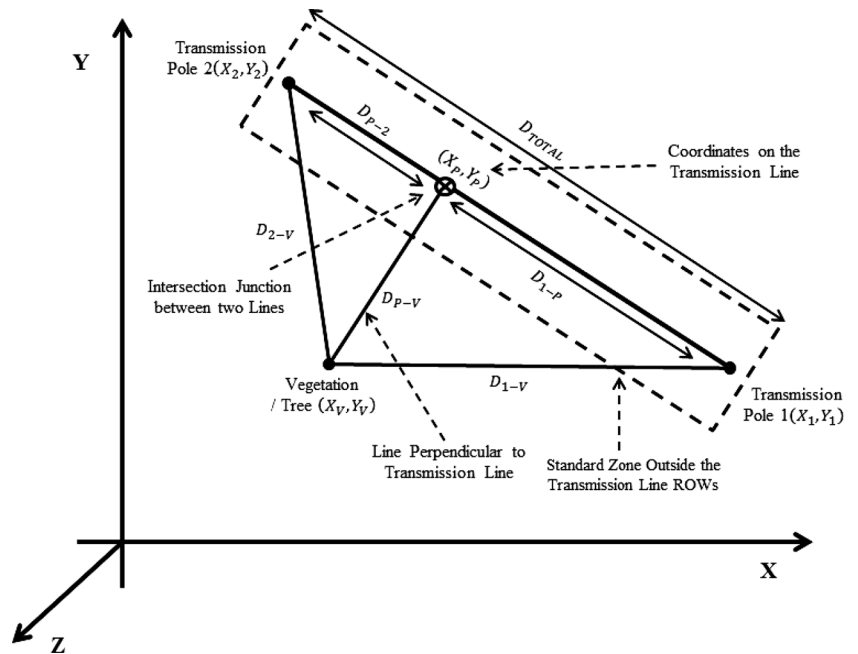


Fig. 19 Model to compute the distance between the HV transmission lines and the encroached vegetations outside ROWs



accurate distance between the encroached vegetation and the HV lines.

Where

- (X_1, Y_1) = Coordinates of the transmission pole 1.
- (X_2, Y_2) = Coordinates of the transmission pole 2.
- (X_V, Y_V) = Coordinates of the vegetation/tree outside ROWs.
- (X_P, Y_P) = Coordinates on the HV transmission lines.
- D_{1-V} = Distance between the vegetation and pole 1.
- D_{2-V} = Distance between the pole 2 and vegetation/tree.
- D_{P-V} = Distance between the vegetation and HV lines.
- D_{1-P} = Distance between the pole 1 and intersection coordinates on HV lines.
- D_{TOTAL} = Distance between two transmission poles.

As shown in Fig. 19, the distance from the encroached vegetation to the HV transmission lines can be calculated by determining the coordinates of the intersection between the two lines. The calculation steps are given below:

The equation for transmission line is given as:

$$m_{TXline} = \frac{Y_2 - Y_1}{X_2 - X_1}, \theta_{TXline} = \tan^{-1}(m_{TXline}) \tag{19}$$

$$Y - Y_1 = m_{TXline}(X - X_1) \tag{20}$$

Equation for estimating perpendicular distance between the encroached vegetation (outside the HV transmission lines) and the HV lines connecting the two transmission poles is given as:

$$\theta_V = \theta_{TXline} - 90^\circ, m_V = \tan(\theta_V) \tag{21}$$

$$Y - Y_V = m_V(X - X_V) \tag{22}$$

The intersection of the two lines is:

$$Y_P - Y_1 = m_{TXline}(X_P - X_1) \tag{23}$$

$$Y_P - Y_V = m_V(X_P - X_V) \tag{24}$$

Subtracting Eq. (23) from (24), we get:

$$Y_V - Y_1 = (m_{TXline} - m_V)X_P + m_VX_V - m_{TXline}X_1 \tag{25}$$

The coordinates (X_P, Y_P) of the respective point on the HV transmission lines is:

$$X_P = \frac{(Y_V - Y_1) - (m_VX_V - m_{TXline}X_1)}{m_{TXline} - m_V} \tag{26}$$

$$Y_P = m_V(X_P - X_V) + Y_V \tag{27}$$

Thus, the distance between the outside vegetation and the HV overhead lines D_{P-V} is:

$$D_{P-V} = \sqrt{(X_V - X_P)^2 + (Y_V - Y_P)^2} \tag{28}$$

The distance between the outside vegetation and the far away pole is given below:

$$D_{2-V} = \sqrt{D_{P-V}^2 + D_{P-2}^2} = \sqrt{D_{P-V}^2 + (D_{TOTAL} + D_{1-P})^2} \tag{29}$$

where $D_{P-2} = D_{TOTAL} - D_{1-P}$.

The coordinates (X_1, Y_1) , (X_2, Y_2) and (X_V, Y_V, D_{1-V}) can be found by using the above triangulation method. By using these coordinates and the respective slopes m_V and m_{TXline} , the coordinates (X_P, Y_P) can be calculated. Therefore, after finding the transmission lines coordinates (X_P, Y_P) corresponding to the vegetation coordinates (X_V, Y_V) as in Fig. 19 distance formula is applied to find out the distance between the transmission lines and the vegetation outside ROWs as in Eq. (29). The equation can also be used to find out the distance between the far away transmission pole 2 (X_2, Y_2) and the vegetation (X_V, Y_V) outside ROWs. Thus, overall status of the vegetation is found by comparing the level (height) of vegetation, and the distance from HV lines. For example, if the level of encroached vegetation outside the HV lines is in danger zone and distance of vegetation from the HV transmission lines is also in danger zone then the overall status of the vegetation encroachment shown by the algorithm would be dangerous and vice versa.

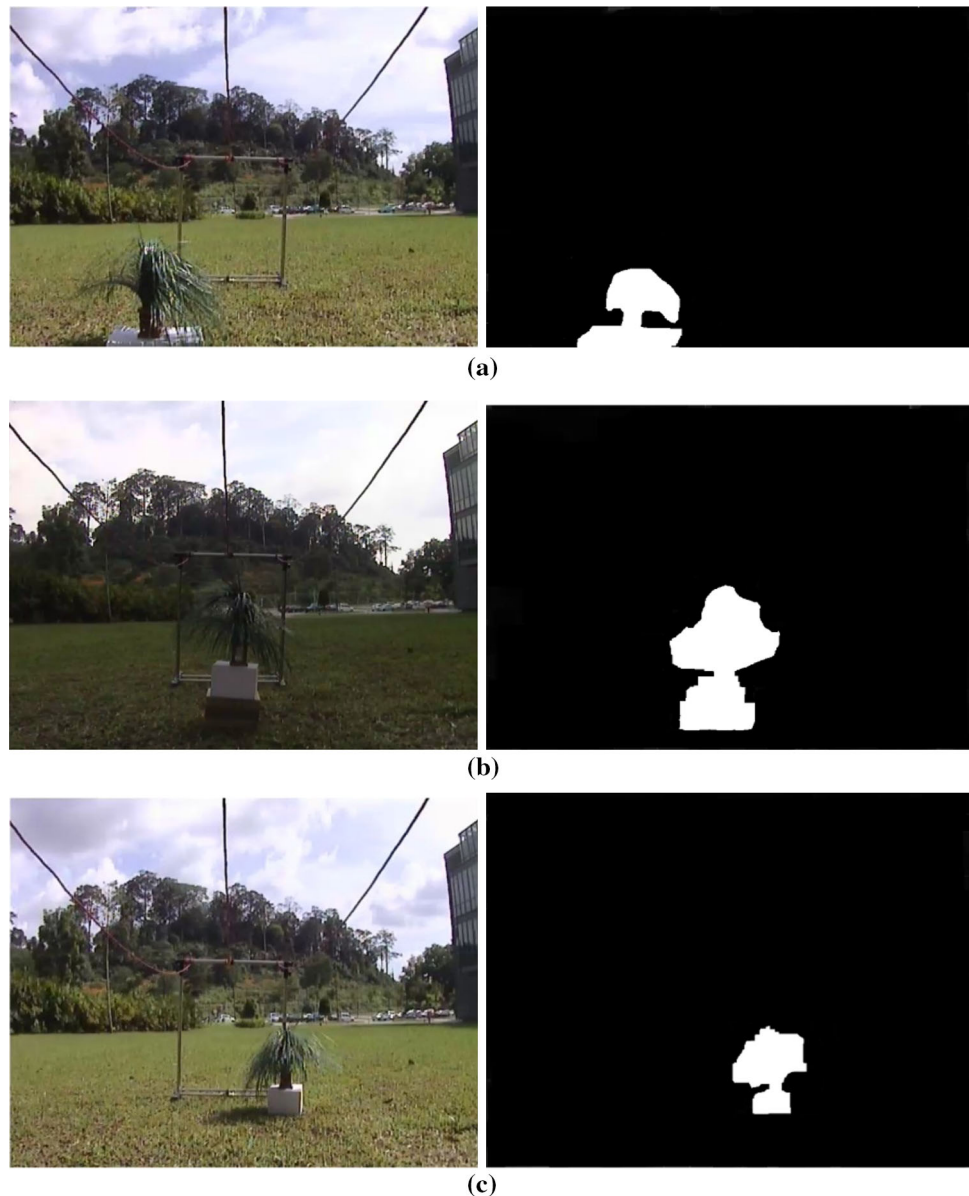
4 Results and discussion

4.1 Testing and validation of proposed method

In order to validate the proposed method, we have carried out a number of tests by making various models of vegetation growth as in Fig. 20. Thus after taking snapshots with clear weather we apply Sect. 3.4 (vegetation tracking using background-subtraction) of methodology which uses horizontal thresholds to find the level of encroached vegetation within and outside ROWs, and also vertical thresholds to ensure a safe clearance from the vegetation in vicinity (outside ROWs). Thus, we are successful in finding overall status of encroached vegetation within and outside ROW for different encroachment scenes. Figure 20a, b and c shows the plant (tree) within ROWs having medium, high, dangerous, and high levels, respectively. But this technique causes ambiguities owing to magnification problems due to the fact that tree of same height near (less distance) the camera appears to be bigger rather than the same tree at a greater distance from the camera. Therefore, we have overcome this problem by placing more number of horizontal and vertical thresholds as in Sect. 3.5 of the methodology.

However, by applying DfT algorithm we can get more accurate results by firstly finding out the distance of tree from both poles (camera pole and the far away pole). The

Fig. 20 Snapshots of various encroachments under different illuminations



results of the vegetation detection are in the form of bottom most point and the top most point of tree as it is shown in Fig. 21 where these two points will be used for depth estimation and computing the height of the tree in the image. The input to the DfT method is in a form of two 2D points which represents the bottom and the top point of the detected tree blob. The DfT algorithm computes the ground location of the tree (in meter) and the distance between the tree and the camera (depth of field). In addition, the algorithm also returns the height of the tree Fig. 22a shows a scene with a tree, where the ground truth (GT) depth (distance) between the tree and the poles is acquired by using a laser range finder (LRF). The Fig. 21b shows the labeled diagram which shows the ground Truth and the computed depth (CD). The vertical angle and height of

camera (external parameters) are calibrated by using plumblines (to measure angle) and with respect to height of pole. For scene in Fig. 22a vertical angle of camera = 86° , height of the camera (pole) = 0.95 m, distance between the two poles = 3.87 m.

The standard distance between the power poles depends upon the transmission line rating [24]. For 33 kV power line, the minimum distance is 90 m, whereas for 500 kV line the minimum distance is 400 m. The ground truth and the computed depth between the camera pole and the tree are 2.43 and 2.39 m, respectively. For far away pole the ground truth distance is 1.44 (3.87–2.43) m, and calculated distance is 1.47 m. If we consider the total distance (3.87 m) between the two poles equals the 400 m (standard distance for HV lines [24]), then calculated distance for

Fig. 21 Detection of top most and bottom most points of a tree

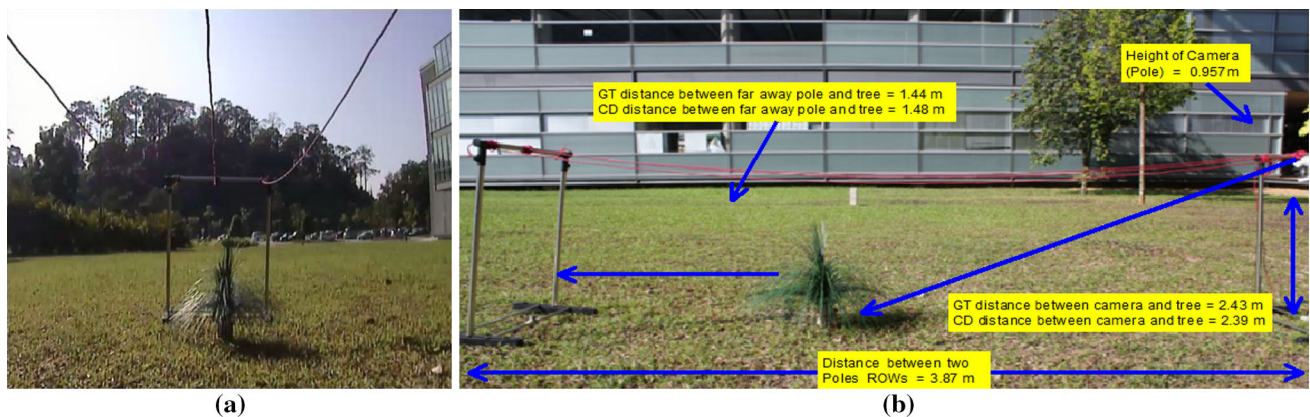
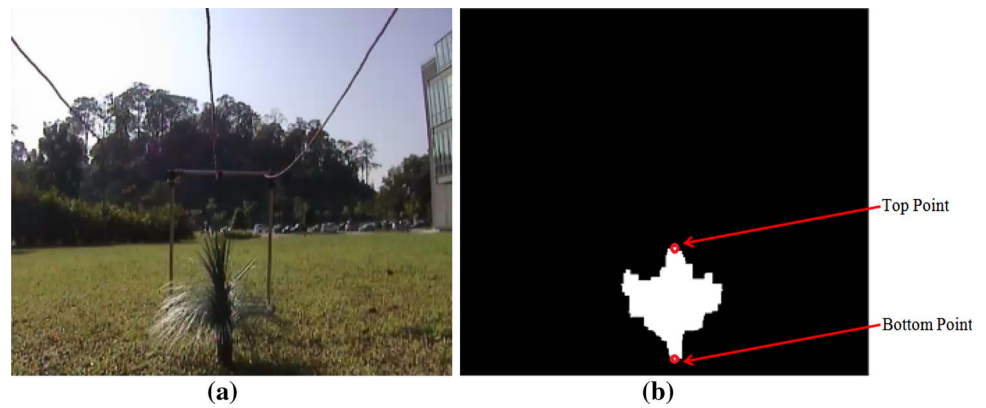


Fig. 22 a Scene containing a tree. b Snapshot showing the GT and the calculated distance between the tree and the poles using DfT

Fig. 21b will be 2.39 m multiplied by factor $(400/3.87 = 103.35)$ which would be 247.95 m for actual HV Overhead line scenario. Table 2 presents different scenes containing tree at a certain distances from the camera (pole) showing XY location, ground truth using laser range finder, calculated distance by applying DfT, and percentage computational error. In Table 2, the scene 4 and 5 shows the tree to be located in front of the far away pole similar to Fig. 16b and having greater ground truth and calculated distance with respect to distance between the two poles.

Similarly, Fig. 23 shows the height of tree calculated in meters as in Sect. 3.5. The ground truth height taken by laser range finder is 0.87 m, and calculated height (CH) is 0.88 m. Table 3 contains the image frames having the tree with different heights. Table 3 shows the calculated depth for base point (BP) and top point (TP) location, ground truth height, calculated height, and the percentage computational error. The standard height of the power poles vary from 15 to 55 m depending upon transmission line rating which can be interpolated with our experimental work to present real time environment as in case of distance between the power poles explained above. Using same steps, the distance between the trees outside ROWs

and the power lines shown in Fig. 24 can be calculated by utilizing the data from DfT. Table 4 contains the image frames having the tree outside ROWs with different distances from power lines.

It is clear from the above results that proposed depth estimation technique has a good computational accuracy. However, there are three sources of possible errors in the proposed method that are; image resolution, camera height, camera pitch angle and the location of vegetation in the image. Other inputs such as image size and field of view are standard and can be obtained from the camera specifications. [25] shows error due to 1 % error in measuring camera height, camera angle or vegetation location. For the tree location 1 % error is relative to the image size. For example, if the image size is (640×480) , 1 % error means 6 pixels error in width and 5 pixels error in height [25] shows a very comprehensive error analysis for these three types of errors. This algorithm is very sensitive to error in the vertical direction compared to the horizontal one. This is because the magnification increases drastically in the vertical direction as compared to the horizontal one. Since the vertical angle is more sensitive to error as compared to height of camera therefore, we have shown the accuracy of

Table 2 Analysis of the depth of scene for encroachments

# Scenes	1	2	3	4	5
Image					
Tree Blobs					
Location in XY plane	(-0.23, 2.11)	(-0.96, 1.41)	(0.79, 1.76)	(0.22, 4.01)	(0.34, 4.48)
GT depth between camera (pole) and tree.	2.37	1.98	2.24	4.24	4.68
CD using DfT	2.32	1.95	2.15	4.12	4.59
% Computational Error	2.10	1.51	4.01	2.83	1.92

**Fig. 23** **a** Frame containing a high tree. **b** Height of the tree in meters closer to the power lines

DfT technique in Fig. 25 for real time scenario as the distance between the HV poles is maximum up to 400 m. Figure 25 shows computed depth to be 244 m for a tree located at 250 m of actual distance owing to 1 % error in vertical angle (which is 2.48 % in case of vertical angle (θ) as presented in [25]) if we use 640×480 resolution camera for HV line monitoring.

4.2 Graphical user interface (GUI) for system

A GUI is developed to monitor the encroaching vegetation/trees that can endanger the HV lines. The real time data (containing reference and scene images of indoors and outdoors) is captured and passed through this GUI embedded with the algorithm explained above. GUI is

Table 3 Analysis for height of the tree

# Scenes	1		2		3		4		5	
Image										
Tree Blobs										
CD for BP and TP location (meters)	Z1	Z2	Z1	Z2	Z1	Z2	Z1	Z2	Z1	Z2
	1.43	3.77	1.79	4.71	2.89	8.51	2.67	10.23	2.73	26.67
GT height of tree using LRF (meters)	0.56		0.57		0.64		0.76		0.91	
CH using DfT (meters)	0.58		0.59		0.62		0.73		0.89	
% Computational Error	3.39		3.50		3.12		3.94		2.19	



Fig. 24 **a** A tree outside ROWs in zone out of danger. **b** A Height level tree that can fall on power line outside ROWs

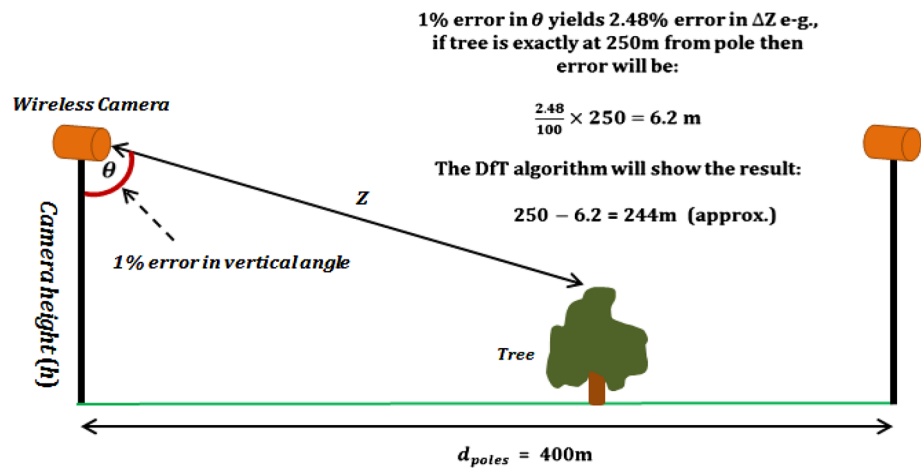
shown in Fig. 26 and it shows the status of tree within and outside ROWs. On the bottom right corner of GUI it can be seen that the user can load the reference and scene

images to get the results. The loaded reference and scene images are displayed at the top middle part of the GUI under heading ‘image display’. The top left part of the

Table 4 Results analysis for distance between tree outside ROWs and power lines

# Scenes	1	2	3	4	5
Image					
Tree Blobs					
Coordinates of Vegetation (X_V, Y_V)	(-2.01, 3.95)	(-1.71, 3.69)	(2.20, 4.47)	(-2.18, 4.48)	(2.67, 3.96)
Coordinates on Power line (X_P, Y_P)	(-0.91, 3.89)	(-0.92, 3.75)	(1.46, 4.39)	(-0.89, 4.51)	(1.34, 3.98)
GT distance between tree outside ROWs and Power lines	1.08	0.81	0.77	1.26	1.36
CD between tree and lines using DfT	1.10	0.79	0.74	1.29	1.33
% Computational Error	1.18	2.46	3.89	2.32	2.20

Fig. 25 Error analysis (for 1 % error in vertical angle) for a tree placed between two HV poles (that are 400 m apart)



GUI shows the data relating to transmission line which includes:

- Transmission Pole Coordinates.
- Transmission Line Rating.
- Temperature.
- Weather Condition.
- Height of the Power line Sag.
- Distance between the two Poles.

Firstly, the transmission pole coordinates will show the latitude and longitude for the location of real-time HV poles installed by electrical utilities at the various locations within the electrical distribution network. After that the transmission line rating shows the pop-up menu to select the rating (including 500, 275, 132, 33, and 15 kV) of HV

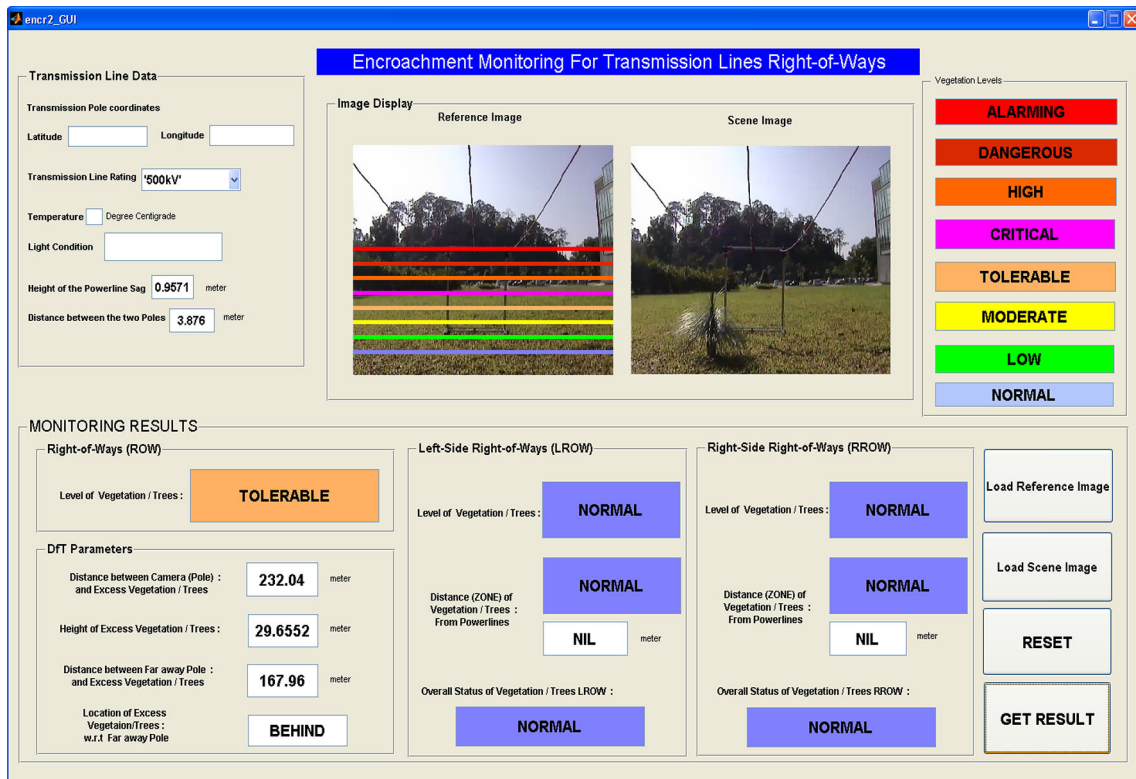


Fig. 26 GUI shows the vegetation encroachments and results

lines as discussed in Sect. 4 of the methodology. The rest of parameters include the temperature, weather condition of the scene, height of the power line sag, and the distance between the two HV poles ROWs. The reference image at the top contains eight horizontal zones (levels) on it presented by different colors as shown at the top right of the GUI.

The last part of the GUI shows the monitoring results within and outside (left or right side) ROWs. For monitoring within ROWs, it shows the level of encroached vegetation/tree e.g., the GUI shows a tree within ROWs in a medium zone. Whereas for monitoring outside ROWs, the GUI shows the level of vegetation, distance between the vegetation and HV power lines, and the overall status of vegetation/trees either at the left or right side of the pole. Whereas, the bottom left part of the GUI shows the DfT parameters which include:

- Distance between the camera (pole) and the tree.
- Distance between the far away pole and the tree.
- Height of the tree.
- Location of excess tree w.r.t. far away pole.

The above mentioned parameters will show the values according to the real-time transmission line standards, e.g. for 500 kV HV lines the GUI shows distance between the camera (pole) and the tree to be 232.04 m,

distance between the far away pole and tree to be 167.96 m, height of the tree to be 29.65 m, and the location of the tree to be behind the far away pole. Therefore, this GUI has great a potential to be utilized for the online monitoring of power line against dangerous encroachments ROWs.

5 Conclusions

In this paper, we have presented a new non-airborne based method that consists of a single wireless cameras integrated on transmission poles ROWs that will transmit the data to base station by communicating with one another. At the base station, images with appropriate illumination (sunny or cloudy weather) will only be used for further processing regardless of rainy and foggy images that will be immediately discarded after identification by predominant pattern recognition methods (which includes: PCA and ‘dark channel prior model’). After that image processing based tracking algorithm is used to detect the vegetation, and a depth from triangulation based method is used that identifies actual 3D coordinates of the encroached vegetation. That helps in locating the accurate height of trees, distance between trees and poles, and distance between dangerous trees and HV lines outside ROWs. On the other hand, the

operators at base station will order the trimmers to cut-off the vegetation wherever it is required. The major advantage of this method is that it requires investment only once for setting up the camera kits. Thus, the use of a single camera proved to be more accurate and less time consuming, as it can provide actual parameters of the scene.

Acknowledgments This research work is supported by Electricity Trust Fund (MESITA), Akaun Amanah Industri Bekalan Elektrik (AAIBE) Grant, Ministry of Energy, Green Technology and Water Malaysia.

References

- Andersson G, Donalek P, Farmer R, Hatzigiorgiou N, Kamwa I, Kundur P, Martins N, Paserba J, Pourbeik P, Sanchez-Gasca J, Schulz R, Stankovi A, Taylor C, Vittal V (2005) Causes of the 2003 major grid blackouts in North America and Europe, and recommended means to improve system dynamic performance. *IEEE Trans Power Syst* 20:1922–1928
- J. Ahmad, Aamir S. Malik, L. Xia (2011) “Effective techniques for vegetation monitoring of transmission lines right-of-ways,” *IEEE International Conference on Imaging Systems and Techniques*, Penang, Malaysia, pp. 17–18 34–38
- Ahmad J, Malik AS, Xia L, Ashikin N (2013) Vegetation encroachment monitoring for transmission lines right-of-ways: a survey. *Electr Power Syst Res* 95:339–352
- Duller A, Whitworth C, Jones DI, Earp GK (2001) Aerial video inspection of overhead power lines. *IET Power Eng J* 15(1): 25–32
- Jones DI, Earp GK (2001) Camera sightline pointing requirements for aerial inspection of overhead power lines. *Electr Power Syst Res* 57:73–82
- Mclaughlin RA (2006) Extracting transmission lines from airborne LIDAR data. *IEEE Geo-Sci Remote Sensing Lett (GSR)* 3:222–226
- Sun C, Jones R, Talbot H, Wu X, Cheong K, Beare R, Buckley M, Berman M (2006) Measuring the distance of vegetation from power lines using stereo vision. *ISPRS J Photogramm Remote Sens* 60:269–283
- Mills SJ, Castro MPG, Li Z, Cai J, Member S, Hayward R, Mejias L, Walker RA (2010) Evaluation of aerial remote sensing techniques for vegetation management in power-line corridors. *IEEE Trans Geo-Sci Remote Sens (TGRS)* 48:3379–3390
- Akyildiz IF, Melodia T, Chowdury KR (2007) “Wireless multimedia sensor networks: a survey.” *IEEE Wireless Comm* 32–39
- Yang Y, Lambert F, Divan D (2007) “A survey on technologies for implementing sensor networks for power delivery systems.” *IEEE Power Eng Soc General Meeting*
- Erol-Kantarci M, Mouftah HT (2011) “Wireless multimedia sensor and actor networks for the next-generation power grid.” *Ad Hoc Networks* 9:542–511
- Hirakawa AR, Martucci M, Vilhena CG, Amancio SM, Jose CV (2010) Lemos, “Wireless image transmission in electric power hostile environment”, *IEEE 35th Conference on Local Computer Networks*, Denver, USA, pp.760–763, 10–14
- Corke P, and Wark T (2007) “Long-duration solar-powered wireless sensor networks,” *Proceedings of the 4th Workshop on Embedded Networked Sensors Systems*, pp. 33–37
- Kurihata H, Takahashi T, Ide I, Mekada Y, Murase H, Tamatsu Y, Miyahara T (2005) “Rainy weather recognition from in-vehicle camera images for driver assistance,” *IEEE Proceedings Intelligent Vehicles Symposium*, pp. 6–8, 205–210
- Dong N, Jia Z, Shao J, Li Z, Liu F, Zhao J, Peng PY (2011) Adaptive object detection and visibility improvement in foggy image. *J Multimed* 6:14–21
- Hui Liu D, Man Lam K, Sun Shen L (2005) Illumination invariant face recognition. *Pattern Recogn* 38:1705–1716
- Karhunen J (1998) Principal component neural networks-theory and applications. *Pattern Anal Appl* 1:74–75
- (2002) IEEE, National Electrical Safety Code. Piscataway, NJ: IEEE, (ANSI C2-2002)
- Tilawat J, Theera-umpon N, Member S (2010) Automatic detection of electricity pylons in aerial video sequences. *Int Conf Electron Inf Eng* 1:342–346
- Li Z, Liu Y, Walker R, Hayward R, Zhang J (2010) Towards automatic power line detection for a UAV surveillance system using pulse coupled neural filter and an improved Hough transform. *Mach Vis Appl* 21:677–686
- Guerreiro RFC, Aguiar PMQ, Member S (2011) “Connectivity-enforcing Hough transform for the robust extraction of line segments,” *IEEE Transactions on Image Processing*, pp. 1–26
- Nieto M, Cuevas C, Salgado L, Garcia N (2011) Line segment detection using weighted mean shift procedures on a 2D slice sampling strategy. *Pattern Anal Appl* 14:149–163
- Ting Chen Y, Rong Huang C, Ping Hung Y (2007) Efficient hierarchical method for background subtraction. *Pattern Recogn* 40:2706–2715
- Berhad TN “<http://www.tnb.com.my>”
- Yasir S (2011) ‘3D visual tracking using a single camera’, MSc thesis, Universiti Teknologi Petronas